

Adaptive Model Predictive Control (AMPC) for Current Control of Three-Phase Three-Level Inverters

N. Sohrabi Veske^{1,*}, M.R. Nowrozi², M. Sadeghi³

¹ Department of Control, Faculty of Electrical Engineering, University of Science and Technology, Tehran, Iran.

² Department of Power, Faculty of Electrical Engineering, University of Science and Technology, Tehran, Iran.

³ Nadaja Self-Sufficiency Research and Jihad Organization, Tehran, Iran.

ARTICLE INFO	ABSTRACT
<p>Article History: Received 23 July 2022 Received in revised form 25 September 2022 Accepted 5 December 2022 Available online 6 December 2022</p>	<p>Model Predictive Control (MPC) is widely used in power electronics due to its ability to handle multi-variable constraints and optimize control actions in real time. However, its performance heavily relies on an accurate system model, making it sensitive to parameter variations and model mismatches. To address this limitation, this paper proposes a novel Model-Predictive Adaptive Control (MPAC) method for current control in three-phase, three-level voltage source inverters (VSI). The proposed MPAC approach integrates the Recursive Least Squares (RLS) algorithm for online system parameter estimation, eliminating the need for a predefined model and allowing real-time adaptation to changes in system dynamics. The proposed MPAC method is implemented and tested in a MATLAB/Simulink environment, where its performance is analyzed under various operating conditions. Simulation results demonstrate that MPAC achieves fast and precise current tracking, robust disturbance rejection, and significantly reduced harmonic distortion compared to conventional MPC methods. Furthermore, MPAC exhibits superior robustness against system parameter uncertainties, ensuring stable operation even in the presence of load variations and model inaccuracies. By improving adaptability and robustness, the proposed MPAC approach has significant potential for application in a wide range of power electronic systems, including motor drives, renewable energy conversion systems, and grid-connected converters. The findings of this study highlight the advantages of integrating adaptive estimation techniques into predictive control strategies, paving the way for more efficient and resilient power electronic control systems.</p>
<p>Keywords: Three-phase Inverter, System Identification, Predictive Control, Adaptive Control</p>	

1. INTRODUCTION

Adaptive Model Predictive Control (AMPC) has garnered significant interest across diverse control applications. Within the realm of power electronics, AMPC has demonstrated its effectiveness in inverter control

* Corresponding author: Nima.Sohrabi72@yahoo.com

Department of Control, Faculty of Electrical Engineering, University of Science and Technology, Tehran, Iran.



for various motor drives and converter systems [1]. AMPC has also shown effectiveness in achieving accurate current control, reducing common-mode voltage, and improving overall system performance across diverse power electronics applications.

Model Predictive Control (MPC) has gained significant attention in power electronics due to its flexibility, high performance, and ability to handle multivariable systems and constraints [2,3]. MPC has been successfully applied to various power electronic applications, including active front ends, uninterruptible power supplies, and high-performance drives for induction machines [4]. Key elements of MPC include prediction models, cost functions, weighing factors, and optimization algorithms. Despite its computational complexity, the availability of powerful processors has facilitated MPC's implementation in power electronics[3].

Focusing on three-level inverters, Almaktoof et al. (2014) developed a finite control set MPC strategy for achieving fast load current control while balancing DC-link capacitor voltages [5]. Additionally, they presented a robust current control technique using MPC for variable DC-link voltage source inverters in renewable energy systems, showcasing the applicability of MPC in renewable energy applications.

The crucial role of three-phase inverters in the power supply process of industrial equipment, military devices, and household appliances in various industrial processes is undeniable today [6; 7]. From small-scale applications such as starting a motor to use in power plant transmission lines, all require some type of inverter in their structure. Another important issue that should be mentioned is the growing use of renewable energy sources in the power generation industry. Voltage source inverters [8, 9] have a wide range of applications for connecting wind generators, photovoltaic sources, microturbines, and fuel cells to the grid, and controlling grid-connected inverters is one of the most up-to-date topics in electrical engineering. On the other hand, line faults or power outages, voltage drops, overcurrents, total harmonic distortions [10], etc., are always a serious problem for electrical and electronic equipment. As a result, the inverter control system plays a very key role in its efficiency and in dealing with various uncertainties, disturbances, etc. Current control of inverters has several advantages over voltage control. Controlling the injected current to the load results in better efficiency, safety, and stability, and it also provides inherent protection against short circuits.

Various methods have been introduced so far for current control of three-phase inverters [9]. The hysteresis control method [11] has a simple algorithm and easy implementation. Its performance is also acceptable due to its fast dynamic response. However, in the case of three-phase inverters, due to the inter-phase interference, the error may not necessarily be within the hysteresis band. Also, the switching frequency [12] in this method is variable and can lead to higher losses and power losses. In addition, due to the analog nature of this method, its implementation in the digital domain requires a high sampling frequency to ensure that all control variables are within the hysteresis band [10]. Although in [11] this method has been generalized and the hysteresis band is updated in each step, and in [12] fuzzy logic is used for this purpose, the changes in switching frequency are still noticeable. Linear methods; the most famous of which is proportional-integral (PI) control [13], although they have a constant switching frequency, have a significant steady-state error in tracking the sinusoidal input. This error can increase with increasing reference current frequency and in some cases can lead to instability [13]. Other methods such as deadbeat control [14] and resonant proportional control [15] have also been used for current control of three-phase inverters. However, since these methods are highly dependent on the system model and parameters, and the slightest uncertainty in the system can cause their performance to be faulty, they face serious challenges in practical applications [14, 15]. Model predictive control [8] has been widely used in various industries due to its many advantages. However, one of the serious problems with this control method is the correct and accurate modeling of the system under control, which can be a very time-consuming and difficult task in some cases.

This research evaluate Adaptive Model Predictive Control (AMPC) for current control in three-phase three-level inverters. Our method leverages the Recursive Least Squares (RLS) algorithm to achieve online system parameter estimation. This eliminates the need for a pre-defined model and allows the control strategy to adapt to real-time system variations. The proposed model-predictive adaptive control (MPAC) method is implemented and evaluated in a MATLAB/Simulink environment. Simulation results demonstrate the effectiveness of MPAC in achieving: fast and accurate current tracking, robust disturbance rejection and low harmonic distortion under various operating conditions. This paves the way for potential application of MPAC to broader power electronic systems, including motor drives and grid-connected converters.

2. METHOD

The evaluation methodology employs a four-step approach. First, a conventional model predictive control (MPC) strategy is implemented on the inverter system (Section 3) to serve as a baseline for comparison. Next, Section 4 introduces the core of this research - the proposed model-predictive adaptive control (MPAC) method, providing a detailed explanation of its design principles and key features. Subsequently, Section 5 presents extensive simulations conducted within a MATLAB environment to assess the performance of both control strategies. This section includes the simulation setup, parameters, and a thorough analysis highlighting the effectiveness of MPAC. Finally, Section 6 concludes the research by summarizing the key findings and discussing the advantages of MPAC compared to conventional MPC, along with its potential applications in power electronics systems.

3. MODEL PREDICTIVE CONTROL FOR CURRENT CONTROL OF THREE-PHASE INVERTERS

Model predictive control (MPC) is an advanced control method that has been used in various industries since the 1980s. The use of basic control concepts in design, simple controller tuning, the ability to develop for complex systems, easy implementation of control law, considering various constraints and limitations in design, etc. are among the advantages of this controller that has made it widely used in various industries. The interesting point about this controller is that, unlike other control methods whose basic concepts are developed in academic environments, this control strategy has entered academic discussions from the industry, which shows the applicability of this method. In MPC, extracting an appropriate model of the system is crucial for maintaining closed-loop stability and its proper performance. This is because in this method, the system model is responsible for predicting the control output. Therefore, the starting point of MPC design is system modeling.

3.1. SYSTEM MODEL

For modeling, according to [8], assume that a three-phase star resistive-inductive load is connected to the output of the inverter under consideration (Figure 1). As mentioned earlier, the goal is to control the output current of the inverter so that the current is injected into the load with the appropriate amplitude and frequency. According to Figure 1, the inverter power circuit consists of dc devices. Therefore, it can be modeled as a gain. The dynamic model of the inverter can be the output filter in voltage control mode or the load connected to it in current control mode. Since the goal in this article is current control, the system model refers to finding the model of the three-phase load connected to the inverter so that the current of the next moments (with respect to the desired horizon) can be predicted based on it.

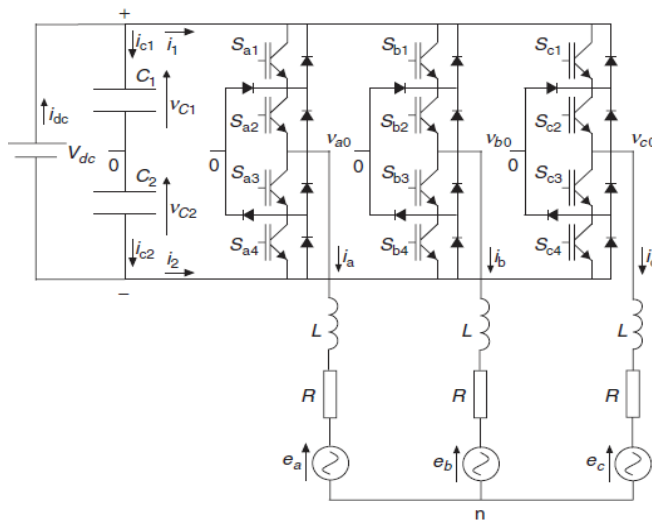


Fig. 1. Three-phase three-level voltage source inverter connected to a resistive-inductive load [8].

In Figure 1, each power switch can have two states: on or off. On means allowing current to flow, and off means preventing current flow. Therefore, the total number of possible states for six switches would be $2^6 = 64$. However,

some of these states are invalid or meaningless for the operation of the inverter. For example, consider a state where all the switches in one leg are on (Sa1, Sa2, Sa3, Sa4). In this case, the circuit would be short-circuited, and no voltage would be applied to the load. Additionally, the switches in this type of inverter are complementary pairs. Therefore, upon further examination, it becomes clear that to generate a three-phase AC waveform at the output, the possible states are as shown in Table 1. In this table, the variable "S" represents the switching state for each phase.

Table 1. Switching States of the Inverter [8]

S_{x2}	S_{x1}	S_x	v_{xN}	S_{x4}	S_{x3}
$\frac{v_{dc}}{2}$	0	0	1	1	+
0	0	1	1	0	0
$-\frac{v_{dc}}{2}$	1	1	0	0	-

Consider equation (1), also known as Clarke's transformation [7] (or alpha-beta-zero transformation), which can be written for any set of three-phase variables that have a zero sum.

$$v = \frac{2}{3}(v_{aN} + \alpha v_{bN} + \alpha^2 v_{cN})$$

$$\alpha = e^{j2\pi/3}$$
(1)

In which the unit vector α represents the 120-degree phase difference between each pair of phases. Therefore, using the above relationship, it is possible to move from a three-dimensional space formed by the three voltage vectors of each phase to a two-dimensional space in i,j(alpha and beta) coordinates. Considering the above, for the inverter in Figure 1, there are 27 possible switching states, which result in the production of 19 different voltage vectors. For a better understanding, refer to Figure 2. According to the inverter output voltage relationship; Equation (1), a similar equation can be obtained for the output current of the inverter (Equation (2)).

$$I = \frac{2}{3}(i_a + \alpha i_b + \alpha^2 i_c)$$

$$\alpha = e^{j2\pi/3}$$
(2)

Up to this point in the system modeling, we have modeled the power circuit part, which is a static model. To model the dynamic part, which is the load connected to the inverter, consider equation (3) for each phase of the resistive-inductive load, where represents the back-emf (reaction) voltage of the load.

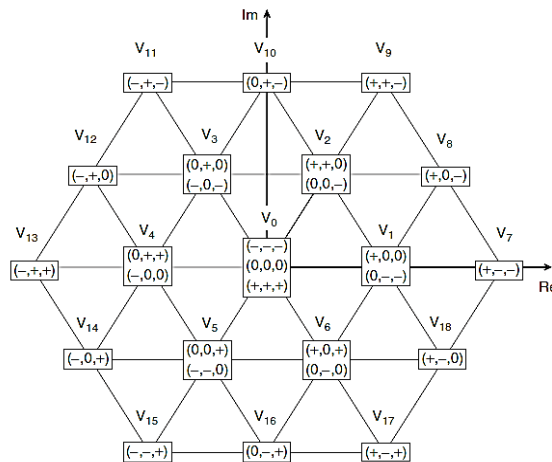


Fig. 2. Possible switching vectors for inverter in Figure 1 [8]

$$\begin{aligned}
 V_{aN} &= Ri_a + L \frac{di_a}{dt} + e_a \\
 V_{bN} &= Ri_b + L \frac{di_b}{dt} + e_b \\
 V_{cN} &= Ri_c + L \frac{di_c}{dt} + e_c
 \end{aligned}
 \tag{3}$$

By substituting (3) in (1) and using (2), we arrive at equation (4).

$$\begin{aligned}
 V &= R\left(\frac{2}{3}(i_a + \alpha i_b + \alpha^2 i_c)\right) + L \frac{d}{dt} \left(\frac{2}{3}(i_a + \right. \\
 &\left. \alpha i_b + \alpha^2 i_c)\right) + \frac{2}{3}(e_a + \alpha e_b + \alpha^2 e_c) = Ri + L \frac{di}{dt} + e
 \end{aligned}
 \tag{4}$$

We know that with an appropriate selection of T_s , equation (5) holds true for defining the derivative of a function:

$$\frac{di}{dt} \approx \frac{i(k+1) - i(k)}{T_s}
 \tag{5}$$

Therefore, if we consider the prediction horizon as one step, we arrive at equation (6) for predicting the current at a given instant, where $v_{_emf}$ represents the back-emf (reaction) voltage of the load.

$$i^p(k + 1) = \left(1 - \frac{RT_s}{L}\right)i(k) + \frac{T_s}{L}(v(k) - \hat{e}(k))
 \tag{6}$$

3.2. COST FUNCTION

The second step in MPC is to define a cost function to obtain the control inputs by minimizing it at each step. Considering the chosen prediction horizon, in the simplest case, the absolute value of the error between the measured current from the load and the desired reference current can be considered as the cost function (Equation7).

$$J = |i_{\alpha}^d(k + 1) - i_{\alpha}^p(k + 1)| + |i_{\beta}^d(k + 1) - i_{\beta}^p(k + 1)|
 \tag{7}$$

The real and imaginary parts of the location vector of the desired current at the $k+1$ th moment are and $i_{\alpha}^d(k + 1)$, $i_{\beta}^d(k + 1)$ The real and imaginary parts are the location vector of the flow predicted by the predictive controller ; at that instant. According to the given explanation, the block diagram of theMPC method can be drawn as in Figure 3.

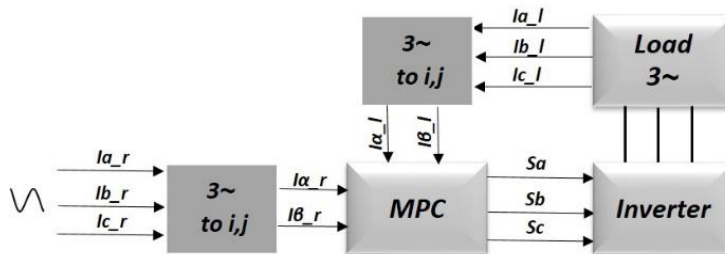


Fig. 3. Block diagram of MPC method

4. MODEL PREDICTIVE ADAPTIVE CONTROL (AMPC)

As we saw in the previous section, the MPC method relies entirely on a model of the system. This algorithm uses the model to predict the value at the next moment (or future moments). Here, the question and challenge arise when: A model of the system is not available, or modeling is very difficult and time-consuming. The values we obtain for resistance and inductance are accompanied by measurement errors, or even if we measure the load parameters correctly, the system parameters become uncertain and change over time due to various reasons, for example, a temperature increase. Our load has capacitive properties in addition to inductance and resistance. We design a model predictive controller for one load, but in practice, we want to connect it to different loads with different parameter values. Therefore, to overcome these challenges, we designed a Model Predictive Adaptive Control (AMPC) strategy for the system in question. In this method, our overall goal is to estimate the load parameters at each step using the input-output data connected to the inverter load and to use the estimated values in Equation (6). Initially, we assume that the load connected to the inverter can be represented by a simple resistive-inductive (RL) model (first-order transfer function).

This assumption is made due to its simplicity and ease of implementation for online parameter identification. If the load also exhibits capacitive properties, these will naturally affect the inductance and resistance values. Consequently, the estimated parameter values will implicitly incorporate the capacitive properties as well. While higher-order models could also be employed, the complexity and computational time required for such models are not suitable for this system due to its fast dynamics. The use of higher-order models would introduce unnecessary complexity and computational burden. The block diagram of the AMPC method is shown in Figure 4.

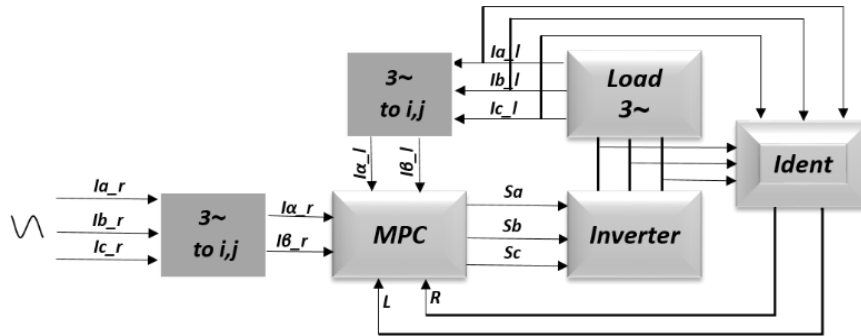


Fig. 4. Block diagram of the methodAMPC

4.1. ONLINE LOAD PARAMETER IDENTIFICATION

The method used for load parameter estimation should be as simple as possible while maintaining desired accuracy and minimizing estimation error. This ensures that the control system under load does not experience computational overload. Therefore, we propose the RLS (Recursive Least Squares) method for this purpose. Details of this method can be found in [16]. Based on the initial assumption, we consider the load structure as given by Equation (3). Neglecting the back-emf voltage and taking the Laplace transform of both sides, we have

$$V = (R + Ls)I \Rightarrow \frac{I}{V} = \frac{1}{Ls + R} \tag{8}$$

As we can see, the time-domain representation of the load equation is a first-order transfer function. Discretizing this equation, we obtain Equation (9). From Equation (9), we can write the discrete-time representation in the form of a first-order ARX model, as shown in Equation (10):

$$G(s) = \frac{R}{Ls + 1} = \frac{a}{\tau s + 1} \Rightarrow G(z) = \frac{a(1 - e^{-\frac{T_s}{\tau}})}{z - e^{-\frac{T_s}{\tau}}} = \frac{az^{-1}}{1 - bz^{-1}} \tag{9}$$

$$I = Y, V = U \Rightarrow \frac{Y}{U} = \frac{az^{-1}}{1 - bz^{-1}} \Rightarrow Y - bz^{-1}Y = az^{-1}U \Rightarrow y(k) = by(k - 1) + au(k - 1) \tag{10}$$

Therefore, by forming the following matrices, the parameter values can be obtained according to the RLS relationship:

$$\theta = \begin{bmatrix} b \\ a \end{bmatrix}, \varphi^T = \begin{bmatrix} y(k-1) \\ -u(k-1) \end{bmatrix}$$

$$\theta(k) = \theta(k-1) + K(k) (y(k) - \varphi^T(k)\theta(k-1))K(k) = P(k)\varphi(k) \tag{11}$$

$$P(k) = \frac{1}{\lambda} (P(k-1) - \frac{P(k-1)\varphi(k)\varphi^T(k)P(k-1)}{\lambda + \varphi^T(k)P(k-1)\varphi(k)})$$

As the equations indicate, another advantage of this method is the ability to update the parameters at each control step. In fact, if the system (in this case, the load connected to the inverter) changes over time, the model parameters will also update themselves accordingly, otherwise they will remain unchanged. In Equation (11), the coefficient [7] represents the forgetting factor, which has a value between zero and one. The closer this parameter is to zero, the more important the previous parameter values are in the update, and the closer it is to one, the more important the current values are in the parameter update. As a result, in the proposed adaptive method, Equation (10) is used instead of Equation (6) to predict the current for the next moment. It should be noted that the back-emf voltage is neglected in the simulations.

5. SIMULATION RESULTS

This section presents the simulation results for both MPC and AMPC methods. The inverter circuit parameters are chosen as $V_{dc}=100v$, $R=1\Omega$, $C=2.2mF$. IGBTs are also used for power switches. As a first test, consider the case where the load connected to the inverter is $R=5\Omega$, $L=5mH$ and the MPC controller is designed for this load. The objective is to track a reference current with frequency $f=50Hz$ and amplitude $I=8A$. The initial parameter values for the AMPC method are chosen as $R=1\Omega$, $L=1mH$. The results for this case are shown in Figures 5 and 6 for the MPC and AMPC controllers, respectively.

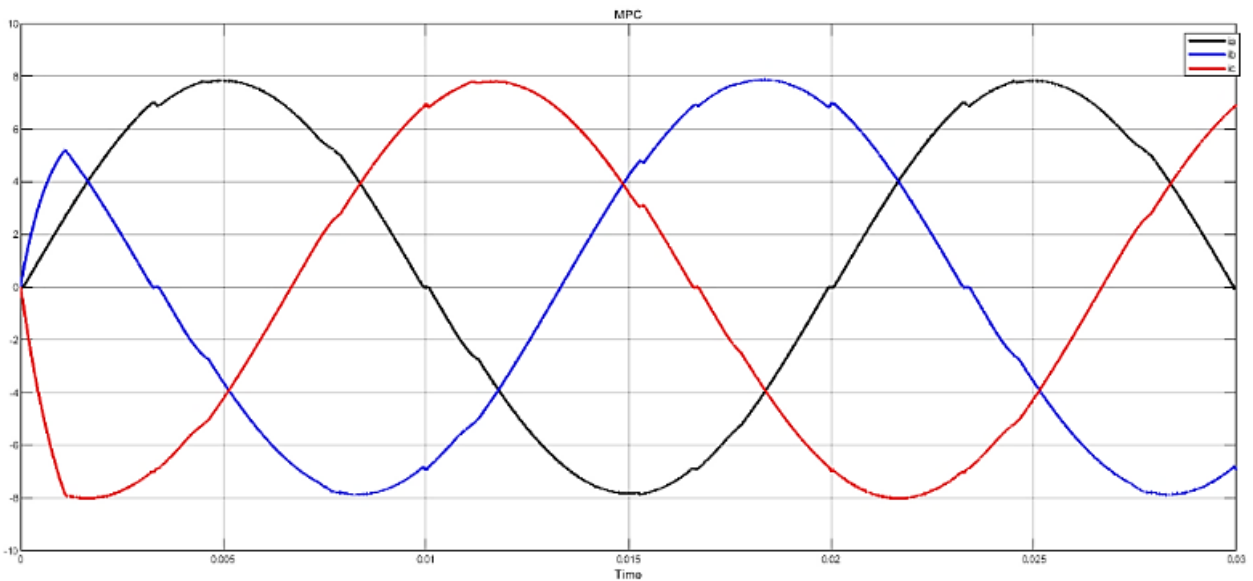


Fig. 5. Load flow diagram for MPC controller $R_l = 5\Omega, L = 5mH$

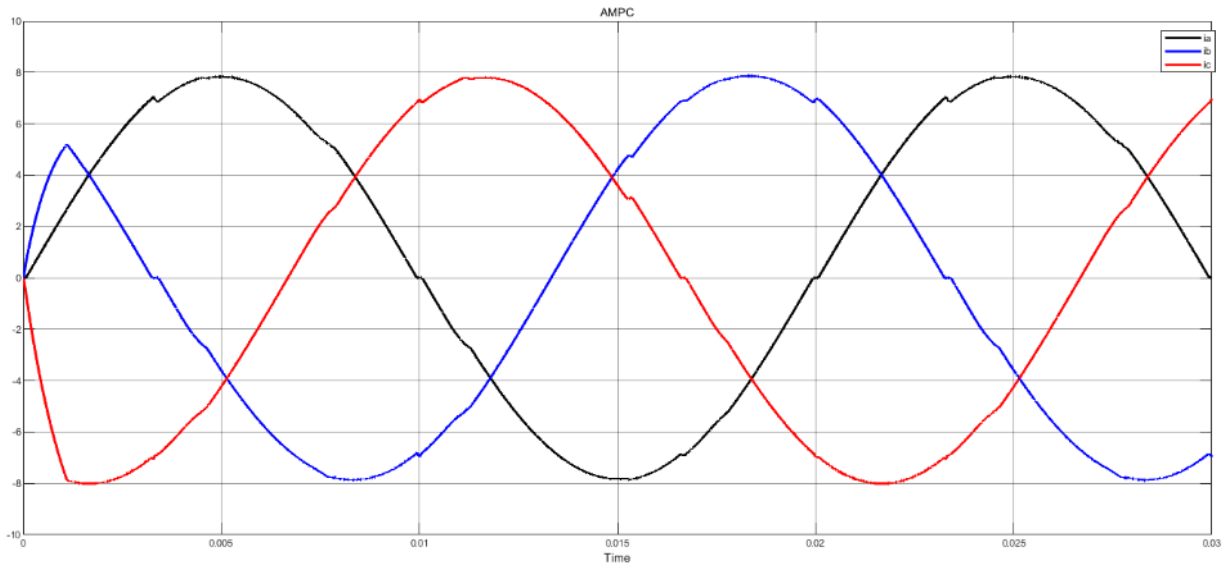


Fig. 6. Load flow diagram for AMPC controller $R_l = 5\Omega, L = 5mH$

As you can see, in this case, both methods have provided appropriate answers. Figure 6 also shows the inductance diagram estimated in the AMPC method is brought. The estimated resistance diagram is similar to this figure .

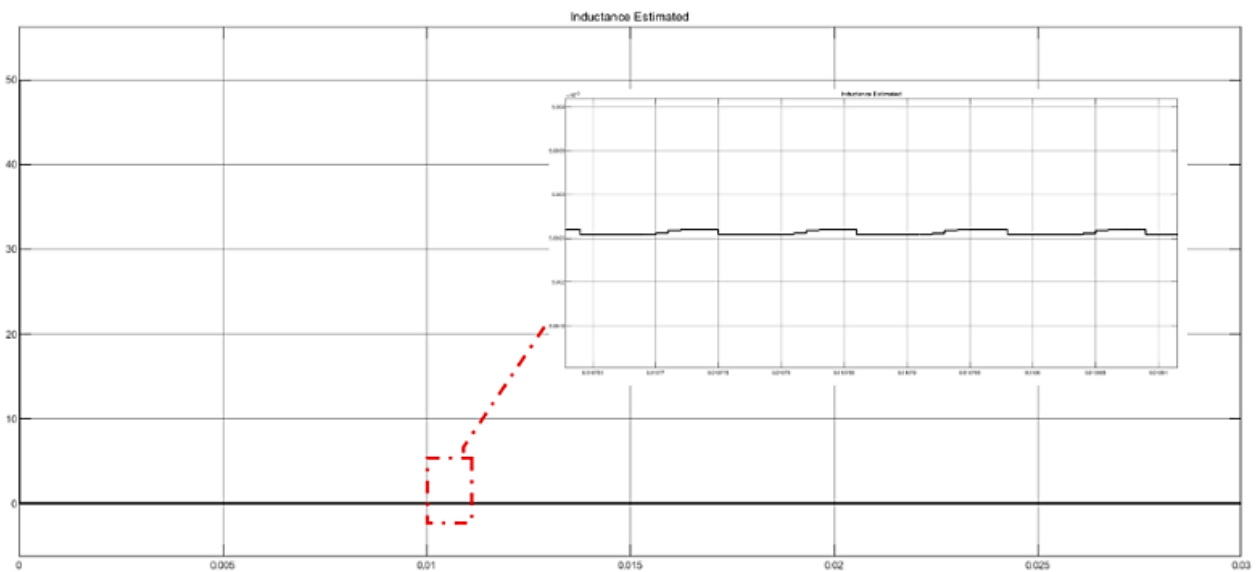


Fig. 7. Estimated inductance diagram for $L = 5mH$ in the method AMPC

For the second test, suppose we have designed the MPC for a load of $R=5\Omega, L=1mH$. But the real load should be equal to $R=3\Omega, L=10mH$. The results related to this mode are shown in Figure 8 for the MPC controller and in Figure 9 for the AMPC controller. As it is clear from the results, the MPC method could not give a good answer in this case where the load parameters have been changed, while the AMPC method had a good performance by updating the parameters. From the standard THD with a value of 1.21% and a current range of 7.8A in AMPC, this good performance is quite evident, in contrast to THD with a value of 12.37% and a current range of 7.3A in the main frequency for MPC. Figure 10 also shows the estimated inductor diagram for this state. To further investigate the effect of changing the load parameters, suppose the load $R=10\Omega, L=10mH$ is connected to the inverter, but the MPC is designed for the load $R=5\Omega, L=5mH$. The results related to this mode are given in Figures 11 and 12 for MPC and in figures 13 and 14 for AMPC. In this case, the time interval of the graphs has been increased to 0.1 seconds for a better comparison. It should also be noted that in this case, because the load impedance

has increased, we have reduced the range of the reference current to $I=5A$ in order to track the reference input current with the same power as the input dc voltage source.

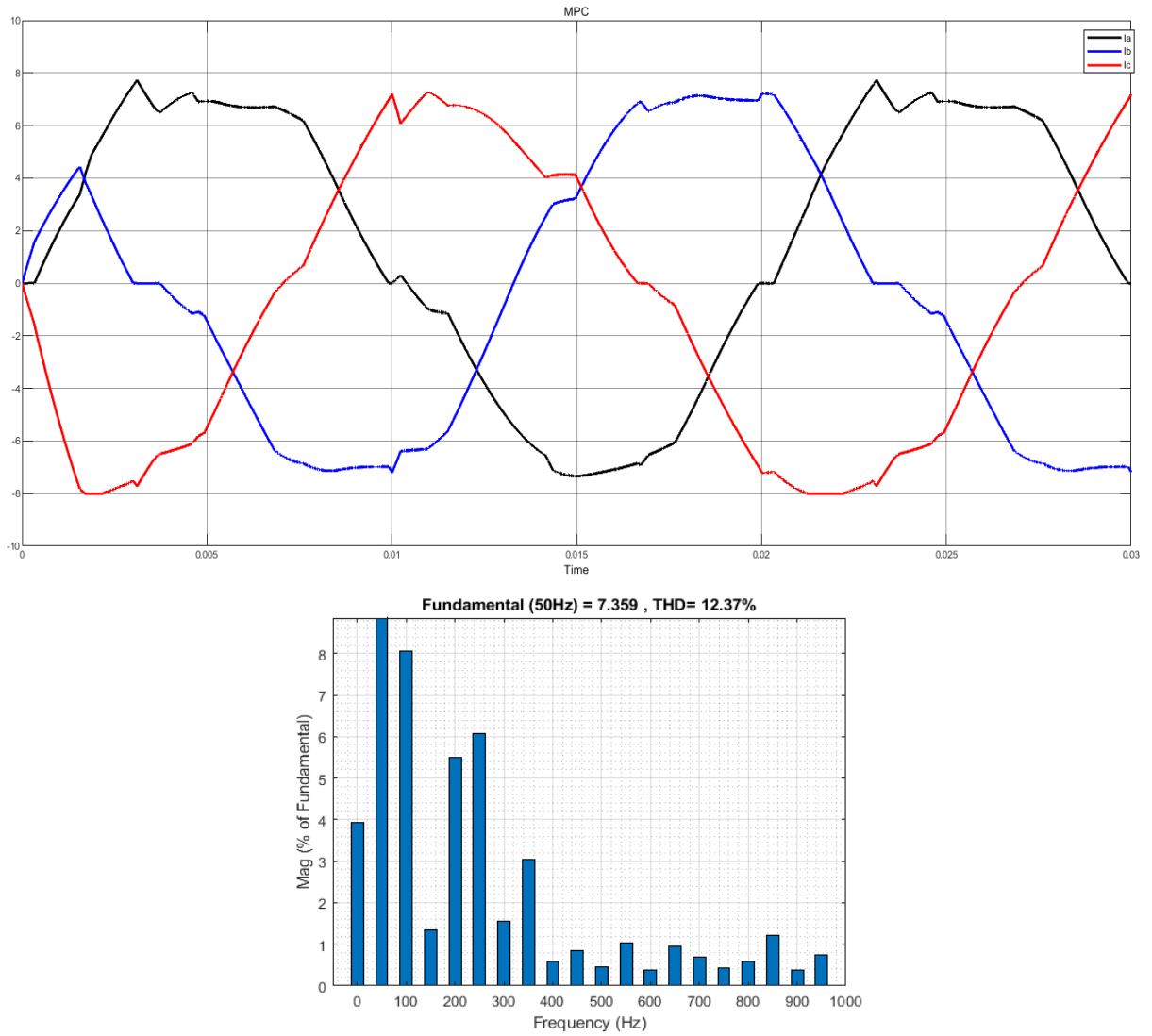


Fig. 8. Load current diagram and its THD for MPC controller $R_l = 3\Omega, L = 10mH$

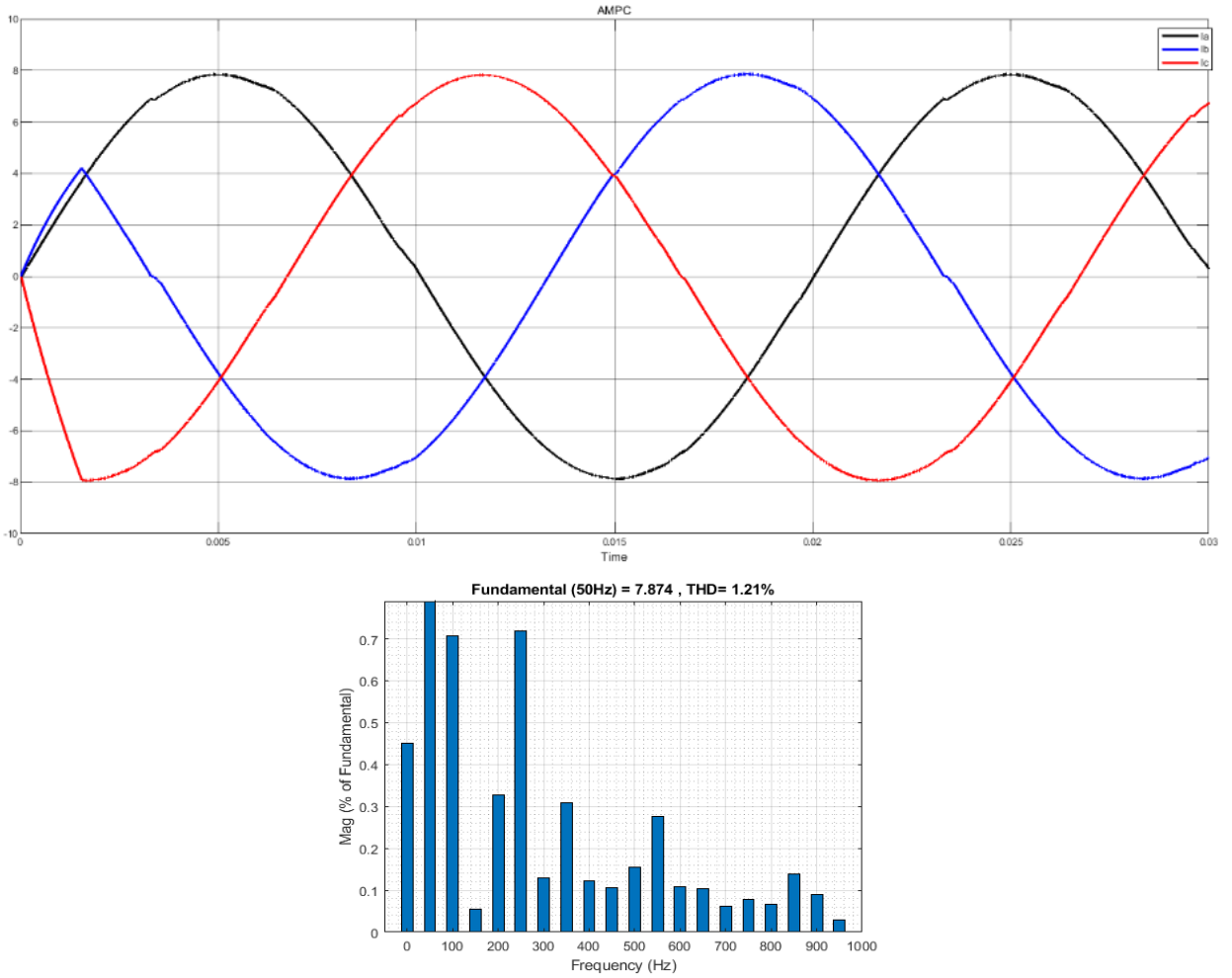


Fig. 9. Load flow diagram and its THD for AMPC controller $R_l = 3\Omega, L = 10mH$

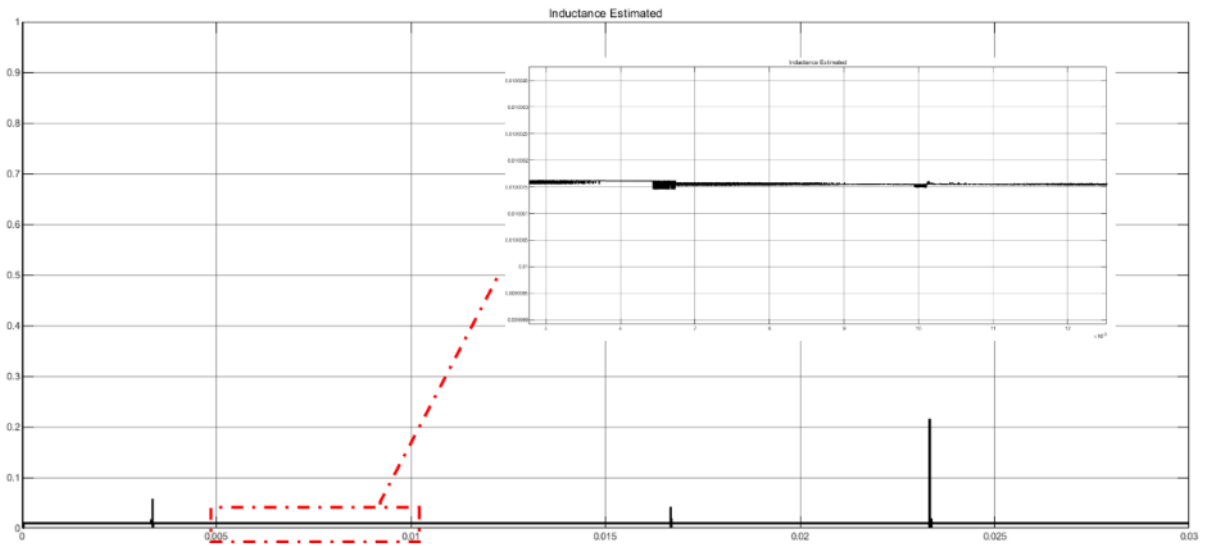


Fig. 10. Estimated inductance diagram for $L=10mH$ in AMPC method

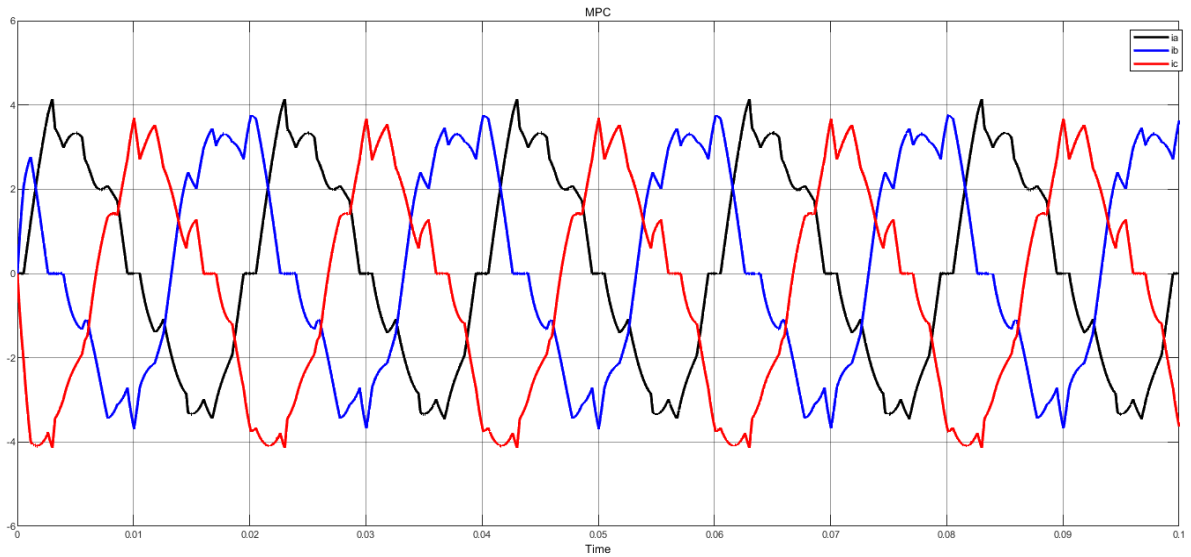


Fig. 11-A. Figure 11-A: Load flow diagram for MPC|5Ω,5mH| controller $R_l = 10\Omega, L = 10mH$

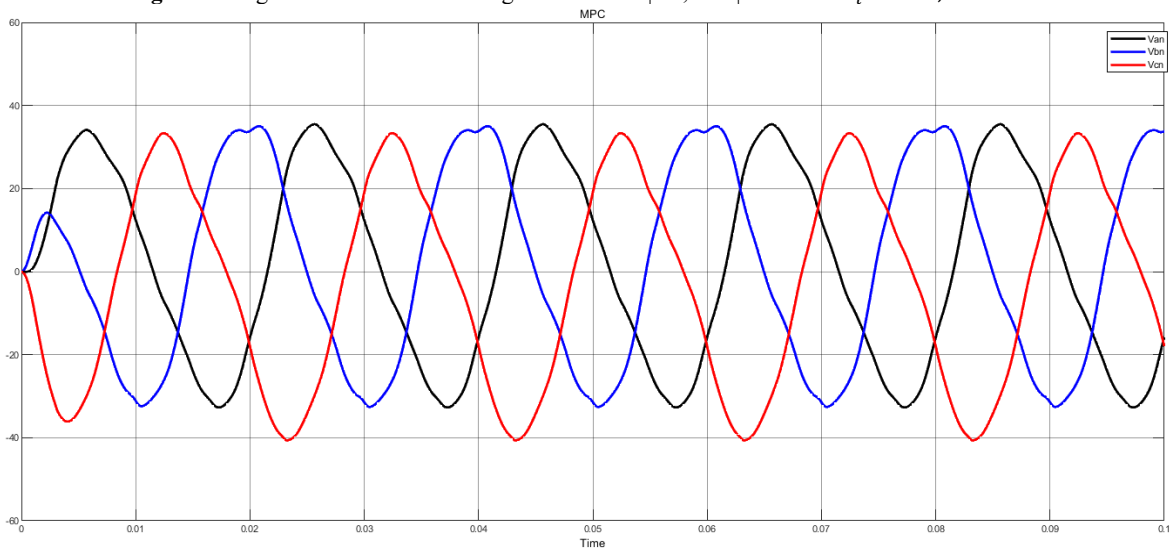


Fig. 11-B. Load voltage diagram for MPC|5Ω,5mH| controller $R_l = 10\Omega, L = 10mH$

the results in this case, we realize that the superiority of the examining ByAMPC method is more noticeable. so that in the flow chart of theMPC method, the value is 22.5% THDi= is seen, while this value is equal toTHDi=1.78% in the AMPC method. Also, this superiority can be seen from the voltage graphs, which passed through a low-pass filter with the same specifications in both methods. Where theMPC controller has resulted inTHDv=14.87% with a value of32.68V at the main frequency and theAMPC controller has a voltage output withTHDv=1.09% and a value of50.61V .at the main frequency

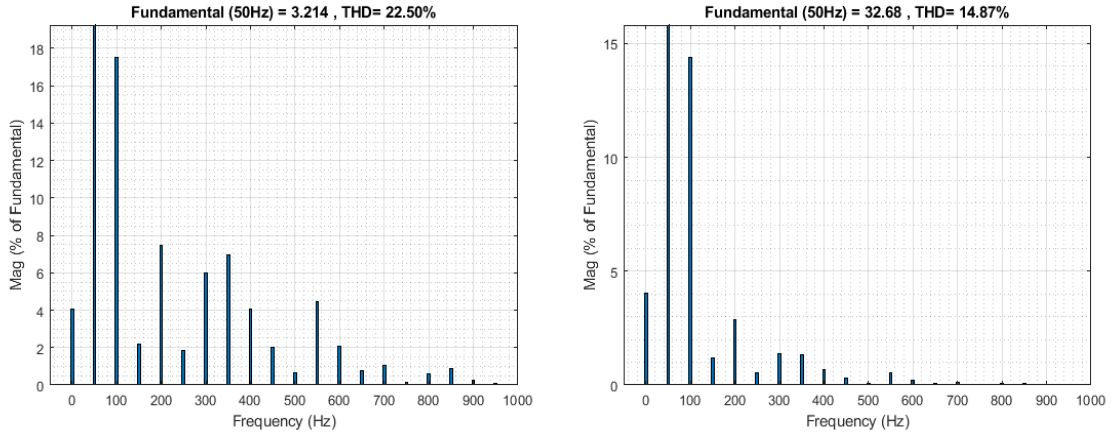


Fig. 12. THD of Voltage (right) and Current (left) of the Load for MPC Controller | $R=5\Omega, L=5mH$ | $R_l = 10\Omega, L = 10mH$

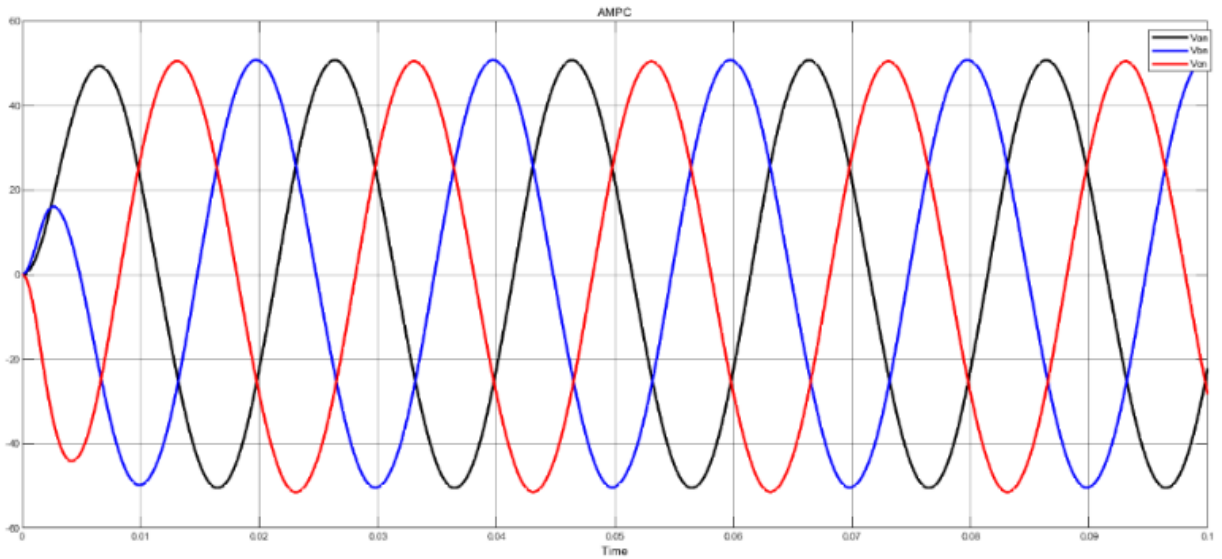


Fig. 13-a. Load flow diagram for AMPC controller $R_l = 10\Omega, L = 10mH$

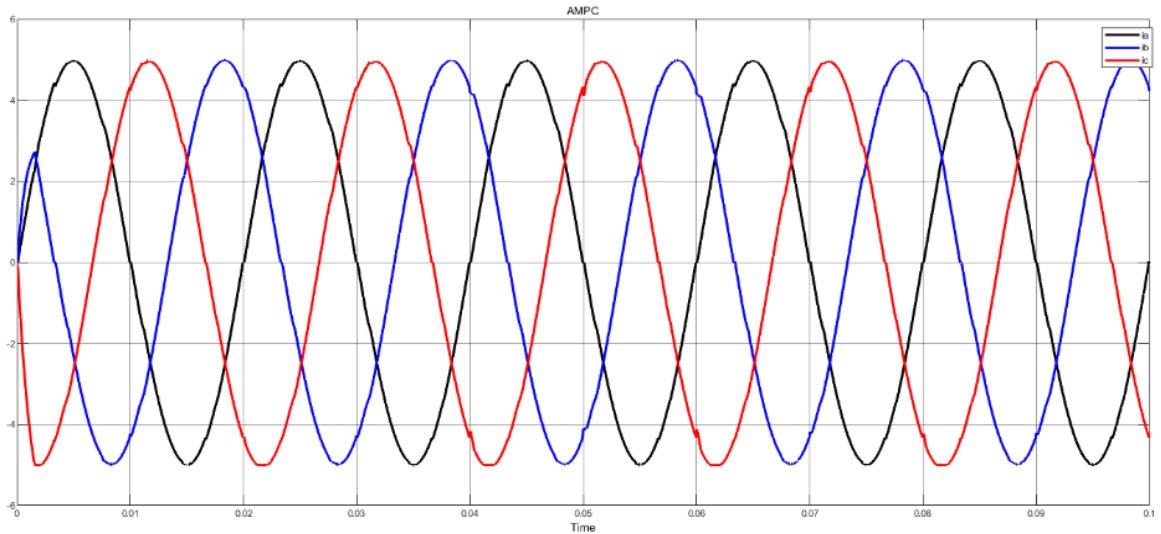


Fig. 13-b. Load voltage diagram for AMPC controller $R_l = 10\Omega, L = 10mH$

In the following, we assume that our load has a viscous property. Therefore, we connect a capacitor with capacity $C=1\text{mF}$ to each phase of load $R=10\Omega$, $L=10\text{mH}$. In this case, we set $V_{dc}=200\text{v}$ and $I_r=10\text{A}$ (reference current range). The results of this mode are shown in Figures 15 and 16. As you can see, in this case, the output of the MPC method has become unstable, but in the AMPC method, we have a relatively favorable output. Although the model for the assumed load is of the 1st order and the actual load is of the 2nd order, but the adaptive method by updating the parameters has been able to perform relatively well in this case.

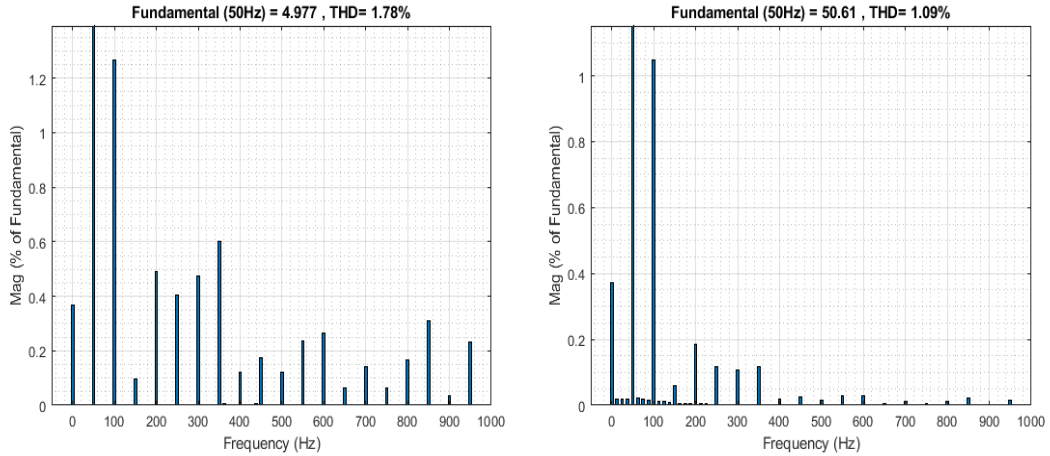


Fig. 14. THD of Voltage (right) and Current (left) of the Load for AMPC Controller | $R_l = 10\Omega$, $L = 10\text{mH}$

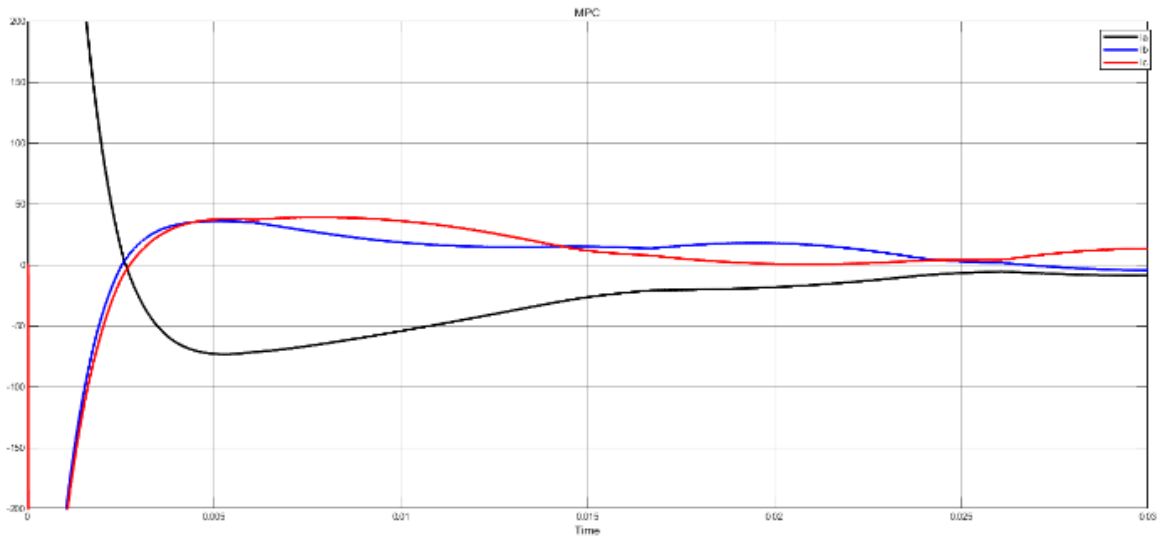


Fig. 15. RLC (resistor-inductor-capacitor) load flow diagram for MPC controller

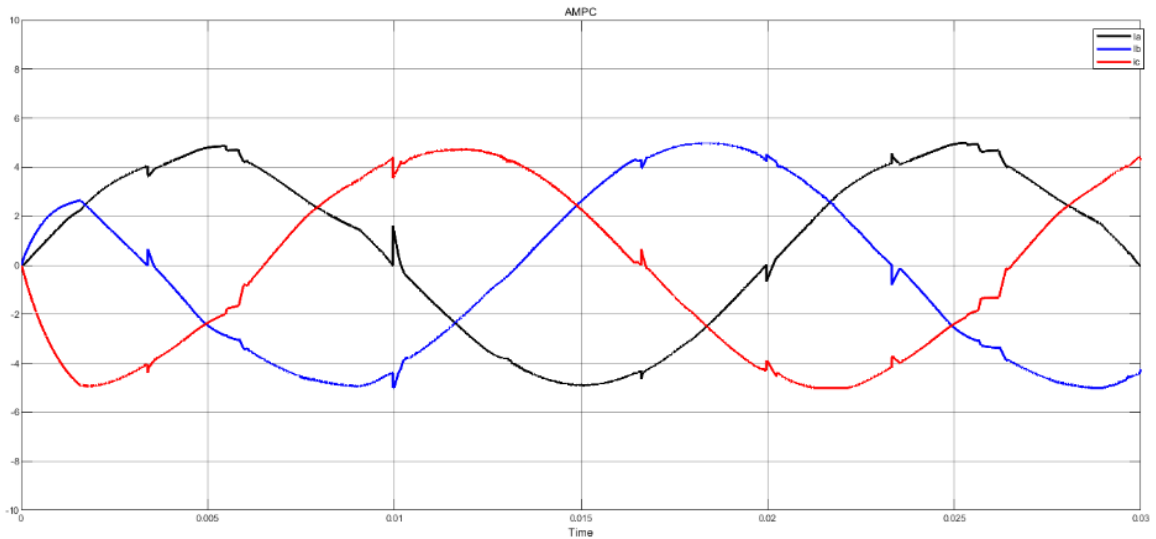


Fig. 16. RLC (resistor-inductor-capacitor) load flow chart for AMPC controller

As a final evaluation, in Figures 17 and 18 the inverter output current traces for applying step changes, of 3A per 0.0015s with the previous parameter values for both methods are given. According to the results, both controllers have performed well against step changes. Of course, with the assumption that the MPC controller is designed precisely for the load and the selection of the initial values of the AMPC method is also appropriate, both methods have performed well in this case.

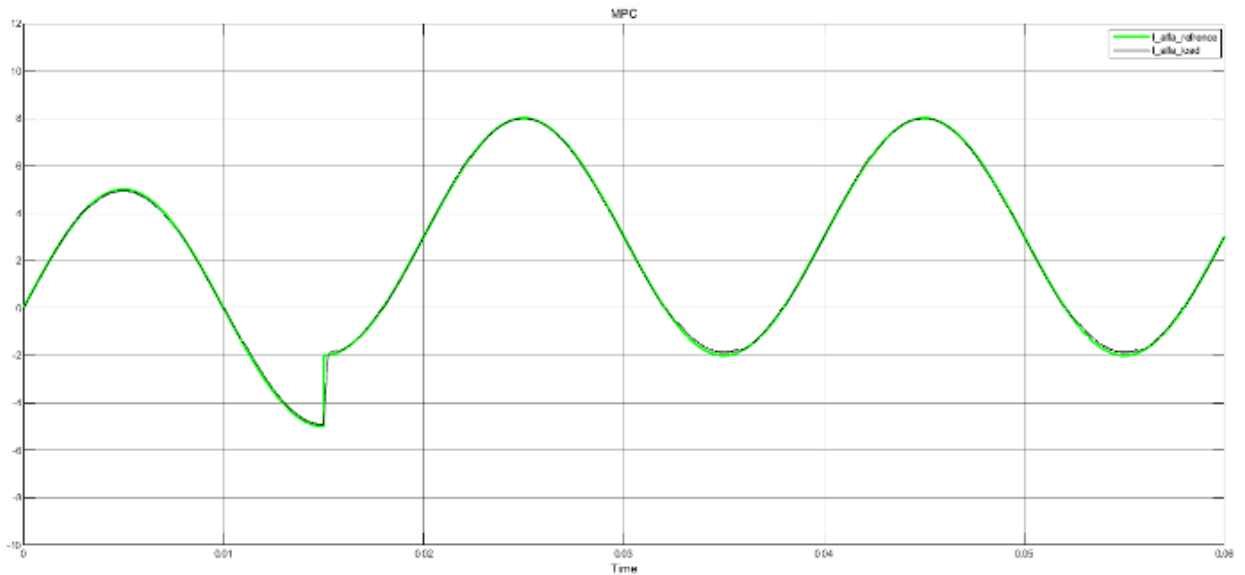


Fig. 17. Tracing step changes in the MPC method. The green diagram of the real component of the reference current after converting three phases to α, β . The black diagram of the real component of the load flow after the aforementioned conversion

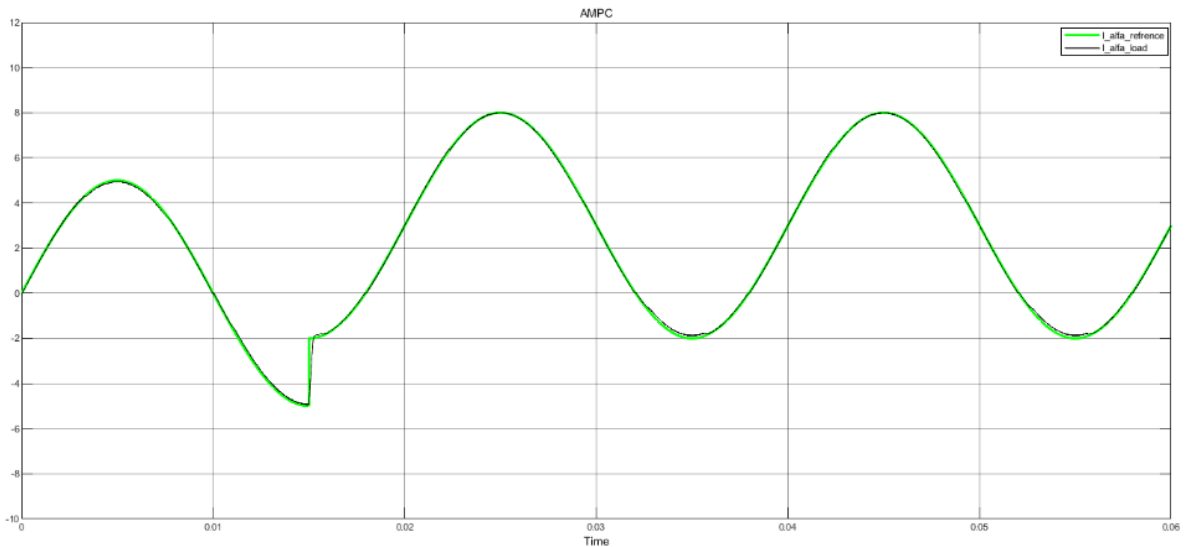


Fig. 18. Tracing step changes in the AMPC method. The green diagram of the real component of the reference current after converting three phases to i_j . The black diagram of the real component of the load flow after the aforementioned conversion

6. CONCLUSION

This study investigated a novel Adaptive Model Predictive Control (AMPC) method with online system identification for power electronics applications. The proposed controller's performance was evaluated through simulations in MATLAB/Simulink and compared to a conventional Model Predictive Control (MPC) strategy. Metrics like Total Harmonic Distortion (THD), reference current tracking, and step input tracking were employed for evaluation. The AMPC method demonstrated superior performance across all metrics, particularly in robustness. Notably, under uncertainties and load parameter changes, the AMPC method achieved a significantly lower THD (THDi = 1.7%) compared to the MPC method (THDi = 22.5%). Moreover, the AMPC method effectively handled loads with unknown dynamics and models, where the MPC controller resulted in unstable output. However, the MPC method benefits from faster execution time due to its pre-defined model. Therefore, for applications with well-defined and known load models, the MPC controller might be preferable. In scenarios with uncertainties, unknown load dynamics, or parameter variations, the AMPC method's robustness and adaptability make it the superior choice. This research offers a valuable control strategy for power electronics, particularly when dealing with uncertainties or unknown load characteristics. The AMPC method's balance between robustness and computational efficiency makes it a promising candidate for a wider range of practical applications.

Transparency Statement

The data supporting this study are available upon reasonable request to the corresponding author, subject to ethical and confidentiality considerations.

Acknowledgments

We would like to express our gratitude to all individuals who contributed to this project.

Declaration of Interest

The authors declare that they have no competing interests.

Funding

This research received no specific grant from any funding agency, commercial, or not-for-profit sectors.

REFERENCES

- [1] Lu, M., Dhople, S., & Johnson, B. B. (2022). Benchmarking nonlinear oscillators for grid-forming inverter control. *IEEE Transactions on Power Electronics*, 37(9), 10250–10266. <https://doi.org/10.1109/TPEL.2022.3162530>
- [2] Borreggine, S., Monopoli, V. G., Rizzello, G., Naso, D., Cupertino, F., & Consoletti, R. (2019). A review on model predictive control and its applications in power electronics. In 2019 AEIT International Conference of Electrical and Electronic Technologies for Automotive (AEIT AUTOMOTIVE) (pp. 1–6). IEEE. <https://doi.org/10.23919/EETA.2019.8804594>
- [3] Alam, M., Ahmad, S., Anees, M. A., Tariq, M., & Azeem, A. (2020). Comprehensive review on model predictive control applied to power electronics. *Current Signal Transduction Therapy*, 13(2), 87–100. <https://doi.org/10.2174/2352096512666191004125220>
- [4] Vazquez, S., Leon, J. I., Franquelo, L. G., Rodríguez, J. R., Young, H. A., Marquez, A., & Zanchetta, P. (2014). Model predictive control: A review of its applications in power electronics. *IEEE Industrial Electronics Magazine*, 8(1), 16–31. <https://doi.org/10.1109/MIE.2013.2290138>
- [5] Almaktoof, A. M., Raji, A. K., & Kahn, M. T. E. (2014). Robust current control technique for variable DC-link voltage source inverters for renewable energy systems. In 2014 International Conference on the Eleventh Industrial and Commercial Use of Energy (pp. 1–6). IEEE. <https://doi.org/10.1109/ICUE.2014.6904206>
- [6] Rohten, J. A., Espinoza, J. R., Muñoz, J. A., Pérez, M. A., Melin, P. E., Silva, J. J., Espinosa, E. E., & Rivera, M. E. (2016). Model predictive control for power converters in a distorted three-phase power supply. *IEEE Transactions on Industrial Electronics*, 63(9), 5838–5848. <https://doi.org/10.1109/TIE.2016.2527732>
- [7] Ravankhah, S. (2014). Three-phase inverter controller design [Unpublished doctoral dissertation]. Iran University of Science and Technology, Tehran.
- [8] Rodriguez, J., & Cortes, P. (2011). Predictive control of a three-phase neutral-point clamped inverter. In *Predictive control of power converters and electrical drives* (pp. 65–79). Wiley. <https://doi.org/10.1002/9781119941446.ch5>
- [9] Rodriguez, J., Pontt, J., Silva, C. A., Correa, P., Lezana, P., Cortés, P., & Ammann, U. (2007). Predictive current control of a voltage source inverter. *IEEE Transactions on Industrial Electronics*, 54(1), 495–503. <https://doi.org/10.1109/TIE.2006.888802>
- [10] Rodriguez, J., & Cortes, P. (2011). Classical control methods for power converters and drives. In *Predictive control of power converters and electrical drives* (pp. 17–30). Wiley. <https://doi.org/10.1002/9781119941446.ch2>
- [11] Harshitha, H. M., Dawnee, S., & Kumaran, K. (2017). Comparative study of fixed hysteresis band current controller and adaptive hysteresis band current controller for performance analysis of induction motor. In 2017 International Conference on Energy, Communication, Data Analytics and Soft Computing (ICECDS) (pp. 121–126). IEEE. <https://doi.org/10.1109/ICECDS.2017.8389497>
- [12] Nasir Uddin, M., & Rebeiro, R. S. (2011). Fuzzy logic based speed controller and adaptive hysteresis current controller based IPMSM drive for improved dynamic performance. In 2011 IEEE International Electric Machines & Drives Conference (IEMDC) (pp. 1497–1502). IEEE. <https://doi.org/10.1109/IEMDC.2011.5994845>

- [13] Liserre, M., Teodorescu, R., & Blaabjerg, F. (2006). Multiple harmonics control for three-phase grid converter systems with the use of PI-RES current controller in a rotating frame. *IEEE Transactions on Power Electronics*, 21(3), 836–841. <https://doi.org/10.1109/TPEL.2006.875566>
- [14] Kukrer, O. (1996). Deadbeat control of a three-phase inverter with an output LC filter. *IEEE Transactions on Power Electronics*, 11(1), 16–23. <https://doi.org/10.1109/63.484412>
- [15] Cha, H., Vu, T.-K., & Kim, J.-E. (2009). Design and control of proportional-resonant controller based photovoltaic power conditioning system. In *2009 IEEE Energy Conversion Congress and Exposition* (pp. 2198–2205). IEEE. <https://doi.org/10.1109/ECCE.2009.5316374>
- [16] Cecati, C., & Rotondale, N. (2002). On-line identification of electrical parameters of the induction motor using RLS estimation. In *IECON '98: Proceedings of the 24th Annual Conference of the IEEE Industrial Electronics Society* (Vol. 4, pp. 2020–2025). IEEE. <https://doi.org/10.1109/IECON.1998.724073>